Assessment of engineering parameters and mass modeling for reducing postharvest losses of sweet lime (*Citrus limetta*) fruit

Shivani Desai[1], Vikram Kad[1], Ganesh Shelke[1], Nashi K. Alqahtani[2,3], Prashant Kumar Patil[4], Sudama Kakade[1], Govind Yenge[1], Sati Y. Al-Dalain[5], Mahmoud Helal[6], Nimah Alnemari[7], Rokayya Sami[7]*, Hala M. Abo-dief[8], Suzan A. Abushal[9], Awatif M. Almehmadi[10], Woroud A. Alsanei[11], Mohamed K. Morsy[12]*

[1]Department of Agricultural Process Engineering, Dr. ASCAE&T, Mahatma Phule Agricultural University, Rahuri, Maharashtra, India; [2]Department of Food and Nutrition Sciences, College of Agricultural and Food Sciences, King Faisal University, P.O. Box 400, Al-Ahsa 31982, Saudi Arabia; [3]Date Palm Research Center of Excellence, King Faisal University, P.O. Box 400, Al-Ahsa 31982, Saudi Arabia; [4]Vice Chancellor, Mahatma Phule Krishi Vidyapeeth (MPKV), Rahuri, Maharashtra, India; [5]Department of Medical Support, Al-Karak University College, Al-Balqa Applied University, Salt, P.O. Box 19117, Jordan; [6]Department of Mechanical Engineering, Faculty of Engineering, Taif University, P.O. Box 11099, Taif 21944, Saudi Arabia; [7]Department of Food Science and Nutrition, College of Sciences, Taif University, P.O. Box 11099, Taif 21944, Saudi Arabia; [8]Department of Science and Technology, University College-Ranyah, Taif University, P.O. Box 11099; [9]Program of Food Sciences and Nutrition, Turabah University College, Taif University, P.O. Box 11099, Taif 21944, Saudi Arabia; [10]Departmentof Clinical Nutrition, Faculty of Applied Medical Sciences, Umm Al-Qura University, P.O. Box 715, Makkah 24382, Saudi Arabia; [11]Department of Food and Nutrition, Faculty of Human Sciences and Design, King Abdulaziz University, Jeddah 21589, Saudi Arabia; [12]Department of Food Technology, Faculty of Agriculture, Benha University, P.O. Box 13736 Qaluobia, Egypt

***Corresponding Authors:** Rokayya Sami, Department of Food Science and Nutrition, College of Sciences, Taif University, P.O. Box 11099, Taif 21944, Saudi Arabia. Email: rokayya.d@tu.edu.sa; Mohamed K. Morsy, Department of Food Technology, Faculty of Agriculture, Benha University, P.O. Box 13736, Qaluobia, Egypt. Email: mohamed.abdelhafez@fagr.bu.edu.eg

Academic Editor: Prof. Massimiliano Rinaldi - Università di Parma, Italy

Received: 12 June 2024; Accepted: 8 October 2024; Published: 1 January 2025

PAPER

Abstract

Lack of data on the engineering properties of sweet lime fruits leads to substantial waste during postharvest processes. This study analyzed the engineering properties of sweet lime fruit, including physical, chemical, thermal, and mechanical properties, and developed mass models to minimize postharvest losses. The average values of the sweet lime's major axis (LA), intermediate axis (IA), and transverse axis (TA), as well as the arithmetic, geometric, and equivalent mean diameters, were 78.71, 77.07, 74.96, 76.92, 76.89, and 76.9 mm, respectively. The mean values of P_{LA}, P_{IA}, P_{TA}, C_{PA}, and S_a were 4663.01, 4567.45, 4444.17, 4558.21, and 18694.41 mm^2, respectively. Sweet lime volumes were measured by V_{ellip}, V_{pro}, and V_{osp}, with average values of 242.95, 254.97, and 249.79 cm^3. The sphericity was 0.95, suggesting that the sweet lime has a spherical shape. The average bulk density and true density were 449.75 and 931.41 kg/m^3. Stainless steel exhibited the minimum static friction. The average peak values of penetration, compression, and cutting forces were 9.44, 311.08, and 148.68 N, respectively. Sweet lime had average L*, a*, and b* values of 58.07, -13.15, and 51.38. Models such as S-curve, power, and quadratic were used to predict the sweet lime mass. The linear and quadratic models exhibited the highest R^2 values for the intermediate axis, geometric mean diameter, and ellipsoidal volume, with 0.93, 0.95, and 0.93, respectively. The quadratic model, based on geometric mean diameter, is recommended for accurately estimating sweet lime mass. The results of this study showed a statistically significant relationship ($\rho < 0.01$) for all properties and models.

ISSN 1120-1770 online, DOI 10.15586/ijfs.v37i1.2655

By analyzing the acquired data, postharvest operations for sweet lime fruit processing can be designed, improved, and developed, leading to increased efficiency and productivity.

Keywords: sweet lime, citrus limetta, engineering properties, mass modeling, postharvest losses

Introduction

Sweet lime (*Citrus limetta*), a member of the Rutaceae family, is a tropical fruit valued for its distinctive balance of sweet and tangy flavor as well as its appealing aesthetic qualities (Mondal *et al*., 2019). It is known for its rich nutritional profile and therapeutic benefits, which include a high concentration of vitamin C, copper, zinc, iron, calcium, potassium, antioxidants, and folic acid (Shariq & Sohail, 2019; Younis *et al*., 2015). Additionally, the juice derived from sweet lime is recognized for its ability to alleviate fatigue and possesses anti-carcinogenic and antibacterial properties. Given its versatility and substantial economic potential, the cultivation of sweet lime varieties plays a significant role in commercial agriculture (Bhaumik *et al*., 2018).

As a perishable fruit, sweet limes require a critical number of postharvest procedures, including sorting, washing, waxing, packing, storage, and transportation (Kumari *et al*., 2020). However, a lack of understanding of the physical, thermal, mechanical, and chemical properties of sweet limes often results in considerable fruit wastage during these postharvest processes (Azman *et al*., 2020; Jahanbakhshi *et al*., 2019; Tewari *et al*., 2019). Among these properties, the physical characteristics of fruits significantly influence the design of equipment and procedures for storage, transportation, sorting, and packing (Birania *et al*., 2022; Pathak *et al*., 2019; Shelke *et al*., 2018). Similarly, the thermal properties of fruits play a vital role in thermal processing operations, such as drying, pasteurization, sterilization, and controlling storage conditions (Barbhuiya *et al*., 2020; Mukama *et al*., 2020; Tewari *et al*., 2019). The textural characteristics of fruits, including compression, penetration, cutting, and crushing forces, are crucial for optimizing packaging, transportation, and processing operations (Murakonda *et al*., 2022; Panda *et al*., 2022). Chemical properties, such as total solids, pH, moisture content, and ascorbic acid, significantly influence fruit quality and, consequently, consumer satisfaction (Barbhuiya *et al*., 2020; Shelke, Kad, Pandiselvam, *et al*., 2023). Postharvest losses of fruits have a substantial impact on both the economy and nutrition (Roumani *et al*., 2024). Optimizing equipment selection and process design can reduce losses, product failures, and equipment breakdowns (Roumani *et al*., 2024; Sanganamoni *et al*., 2024). Therefore, understanding the engineering properties of fruits is essential for the design and development of processes and equipment that optimize the efficiency of postharvest operations.

An analysis of consumer preferences reveals that customers typically prefer fruits that exhibit consistency in both weight and shape (Bibwe *et al*., 2022). Therefore, fruit grading is an essential process based on factors such as shape, size, color, texture, and weight. Size grading is a time-consuming and costly process, making it impractical for fruits with irregular shapes. However, the grading process becomes problematic when fruits have similar shapes but differ in weight (Mahawar *et al*., 2019). Furthermore, mass grading surpasses size grading in efficiency, cost-effectiveness, and accuracy due to its automated fruit sorting methodology. Mass-based grading can be performed by directly measuring the weight of the fruit or using models based on its dimensional characteristics. Understanding the correlation between mass and the physical properties of fruits can enhance the efficiency and precision of grading systems (Pathak *et al*., 2020; Shelke *et al*., 2020). Hence, it is crucial to comprehend the correlation between mass and the major, minor, and intermediate dimensions, as well as the projected areas and volume. Regression analysis is commonly used to develop models that predict the statistical correlation between one or more independent variables and the response factor. Previous studies have extensively used various regression models, including linear, S-curve, power models, and quadratic (Azman *et al*., 2020; Shousha *et al*., 2024). Several studies have investigated mass modeling for various fruits, including sohiong (Vivek *et al*., 2018), chebula fruit (Pathak *et al*., 2019), cantaloupe (Jahanbakhshi *et al*., 2019), gooseberry (Tewari *et al*., 2019), sweet orange (Mahawar *et al*., 2020), belleric myrobalan (Pathak *et al*., 2020), guava (Bibwe *et al*., 2022), strawberry (Birania *et al*., 2022), kadamb (Panda *et al*., 2022), amla (Tomar & Pradhan, 2022), wood apple (Murakonda *et al*., 2022), date fruit (Roumani *et al*., 2024), and oil palm (Sanganamoni *et al*., 2024). Currently, there is a lack of published research on the engineering properties and mass modeling of sweet lime fruit. Therefore, to develop suitable processing methods, a comprehensive investigation of the engineering properties of sweet lime is essential. Accordingly, this study aims to evaluate the physical, chemical, thermal,

and mechanical properties of sweet lime fruit and to identify an appropriate model for predicting its mass.

Materials and Methods

Fresh sweet lime fruit samples were obtained from the Department of Horticulture at Mahatma Phule Agricultural University in Maharashtra, India. The harvested fruits were packed into boxes and delivered to the Process and Food Engineering laboratory. Subsequently, the fruits were washed with water and stored at 10 ± 1 °C and 90 ± 3 % relative humidity to minimize environmental damage. The moisture content of the fruits was measured using a standardized methodology (Pathak *et al.*, 2020). This involved drying six sliced fruits in an oven (Tempo Instruments Pvt. Ltd., Mumbai) at 80°C for 72 hours, after which the initial moisture content was determined. The remaining samples were then used for the experiments.

Morphological properties of sweet lime

The weight of the sweet lime fruits was measured using a digital weighing balance (Indosaw, with an accuracy of 0.001 g, Haryana, India). Equations 1 to 4 were used to calculate the percentages of pulp, peel, seeds, and the pulp-to-peel ratio (Abhishek *et al.,* 2017; Patil *et al.,* 2017).

$$\text{Pulp percentage (\%)} = \frac{(\text{Pulp Weight})(\text{kg})}{(\text{Fruit Weight})(\text{kg})} \times 100 \quad (1)$$

$$\text{Peel percentage (\%)} = \frac{(\text{Peel Weight})(\text{kg})}{(\text{Fruit Weight})(\text{kg})} \times 100 \quad (2)$$

$$\text{Seed percentage (\%)} = \frac{(\text{Seed Weight})(\text{kg})}{(\text{Fruit Weight})(\text{kg})} \times 100 \quad (3)$$

$$\text{Pulp to Peel Ratio} = \frac{(\text{Pulp Weight})(\text{kg})}{(\text{Peel Weight})(\text{kg})} \times 100 \quad (4)$$

Physical properties of sweet lime

The dimensions of the fruits were measured using a vernier caliper (Mitutoyo Corp, Japan) with an accuracy of 0.01 mm. A total of 100 sweet lime fruits were selected for physical analysis. The dimensions of each fruit were measured along three linear axes: the major axis (LA), intermediate axis (IA), and minor axis (TA) (Figure 1).

Meanwhile, using three linear axes, the remaining physical attributes were determined: arithmetic mean diameter ($D_{a,}$ mm), geometric mean diameter ($D_{g,}$ mm), equivalent mean diameter ($D_{e,}$ mm), P_{LA} is projected area perpendicular to major axis (mm^2). While P_{IA} refers to the projected area perpendicular to the intermediate axis (mm^2), whereas P_{TA} is the projected area perpendicular to the minor axis; (mm^2). Additionally, C_{PA} represents the critical projected area (mm^2). The aspect ratio (R_a), sphericity (∅), surface area ($S_{a,}$ mm^2), ellipsoid volume ($V_{ellip,}$ mm^3), prolate spheroid volume ($V_{pro,}$ mm^3), and oblate spheroid volume ($V_{osp,}$ mm^3) were determined using established formulas (Bibwe *et al.,* 2022; Khoshnam *et al.,* 2007;

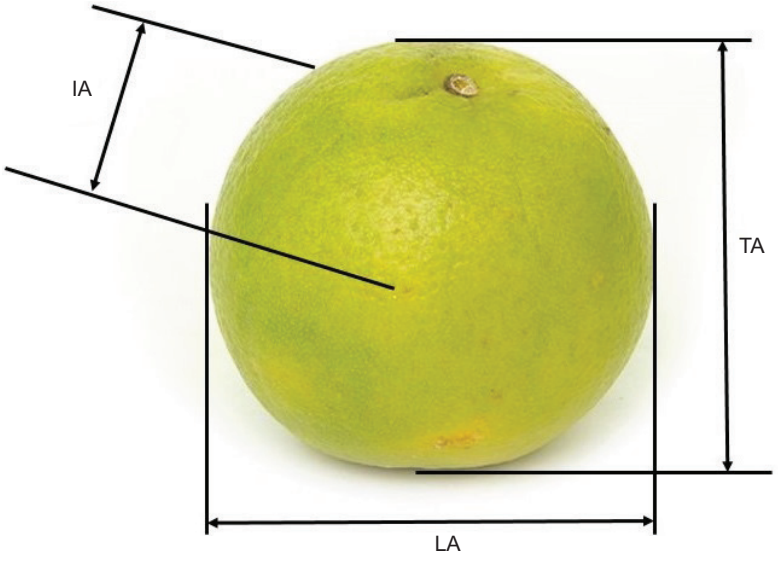

Figure 1. Pictorial view of sweet lime fruit.

Mahawar *et al.,* 2019; Murakonda *et al.,* 2022; Pathak *et al.,* 2020), as shown in Equations 5 and 17.

$$D_a = \frac{LA + IA + TA}{3} \quad (5)$$

$$D_g = (LA \times IA \times TA)^{\frac{1}{3}} \quad (6)$$

$$D_e = \frac{\left\{LA \times (IA + TA)^2\right\}^{\frac{1}{3}}}{4} \quad (7)$$

$$P_{LA} = \frac{\pi \times LA \times IA}{4} \quad (8)$$

$$P_{IA} = \frac{\pi \times IA \times IA}{4} \quad (9)$$

$$P_{TA} = \frac{\pi \times TA \times IA}{4} \quad (10)$$

$$C_{PA} = \frac{P_{LA} + P_{IA} + P_{TA}}{3} \quad (11)$$

$$SA = \pi D_g^2 \quad (12)$$

$$R_a = \frac{IA}{LA} \quad (13)$$

$$\varnothing = \frac{(LA \times IA \times TA)^{\frac{1}{3}}}{LA} \quad (14)$$

$$V_{ellip} = \frac{4\pi}{3} \times \left(\frac{LA}{2}\right) \times \left(\frac{IA}{2}\right) \times \left(\frac{TA}{2}\right) \quad (15)$$

$$V_{pro} = \frac{4\pi}{3} \times \left(\frac{LA}{2}\right)^2 \times \left(\frac{IA}{2}\right) \quad (16)$$

$$V_{osp} = \frac{4\pi}{3} \times \left(\frac{LA}{2}\right)\left(\frac{IA}{2}\right)^2 \quad (17)$$

The bulk density of sweet lime (ρ_b, kg/m^3) was determined using established methodologies (Bibwe *et al*., 2022), while the true density (ρ_t, kg/m^3) was measured using the toluene displacement technique (Murakonda *et al*., 2022). Porosity (ε, %) was calculated using conventional formulas (Tomar & Pradhan, 2022), as shown in Equations 18 and 20.

$$\rho_b = \frac{M_f}{V_b} \quad (18)$$

$$\rho_t = \frac{M_f}{V_f} \quad (19)$$

$$\varepsilon = \frac{\rho_t - \rho_b}{\rho_t} \times 100 \quad (20)$$

where, M_f is the mass of fruits (kg), V_b is the volume of the container (m^3), V_f is the volume of fruit (m^3), which represents the volume of toluene displaced.

Frictional characteristics of sweet lime

The frictional characteristics of the fruit, such as the static coefficient of friction (μ) and the angle of repose (α), were assessed using the methodologies proposed by Pathak *et al*. (2020) and Murakonda *et al*. (2022), respectively. The static coefficient of friction was determined by conducting experimental trials on various surfaces, including rubber, plywood, stainless steel, and aluminum sheets. The static coefficient of friction was calculated using Equation 21, while the angle of repose was determined using Equation 22.

$$\mu = \tan\alpha \quad (21)$$

$$\alpha = \tan^{-1}\left(\frac{2H}{D}\right) \quad (22)$$

where, D refers to the plate diameter (mm), H refers to the heap height(mm).

Thermal characteristics of sweet lime

The specific heat, thermal diffusivity, thermal conductivity, and latent heat of fusion of sweet lime fruit were determined using established mathematical models suggested by Barbhuiya *et al*. (2020) and Vivek *et al*. (2018), as shown in Equations 23 and 26.

$$C_p = 1.667 + 0.025M \quad (23)$$

$$\alpha = \frac{K}{\rho C_p} \quad (24)$$

$$K = 0.148 + 0.00493M \quad (25)$$

$$\lambda = 335\ W \quad (26)$$

Where, C_p is specific heat (KJ/kg °C), M is moisture content (%), K is thermal conductivity (J/m s °C), α is the thermal diffusivity (× 10^{-7} m^2/s), ρ is true density (kg/m^3), λ is the latent heat of fusion (J/kg). These models were developed based on moisture content of fruit. To use these mathematical models, the fruit moisture content must be greater than 60 %.

Mechanical characteristics of sweet lime

The texture properties of the fruits, such as penetration, compression, and cutting, were evaluated using a universal testing machine (AG-X, Shimadzu Analytical, India) equipped with various stainless-steel probes and a 1000 N load cell. The experiments were conducted using established methodologies previously utilized by multiple researchers (Barbhuiya *et al*., 2020). The penetration test was performed using a cylindrical probe with a 6 mm diameter. The fruit sample was initially placed on a lower horizontal surface, and the probe was then moved at a speed of 1 mm/s to a depth of 10 mm. Each fruit was pierced from all four directions. For the compression test, a stainless-steel probe with a circular flat shape and a diameter of 75 mm was used to assess the compressive force. The fruit was subjected to compression at a speed of 1 mm/s, resulting in a maximum deformation of 20%. For the cutting test, a knife probe with a fixed blade was employed. The probe was operated at a speed of 1 mm/s, and the resistance to the depth of the incision was continuously measured. A force-displacement curve was generated for each test, with the force being recorded at every incremental displacement.

Chemical characteristics of sweet lime

Protein content was quantified using the Kjeldahl method, with a correction factor of 6.25 applied (Yıldız *et al*., 2015). The ash content was measured by exposing the sample to a muffle furnace set at a temperature of 550°C (Barbhuiya *et al*., 2020). Fat content was determined using the solvent extraction technique with petroleum ether as the solvent (Hacıseferogulları *et al*., 2007). Carbohydrate content was calculated by subtracting the combined mass of protein, ash, fat, and other discernible constituents from the total mass (Hacıseferogulları *et al*., 2007). The vitamin C content in the fruit sample was determined using the AOAC method 967.21. The sample was homogenized, extracted with metaphosphoric-acetic acid, filtered, and titrated with 2,6-dichloroindophenol (DCPIP) until a pink color appeared. The vitamin C content was calculated based on the volume of DCPIP used and expressed in mg per 100 g of the sample (Barbhuiya *et al*., 2020). Fiber content was analyzed according to Hacıseferogulları *et al*. (2007). The pH and total soluble solids in the fruit juice were measured using a digital pH meter (ELICO Ltd., Hyderabad, India) and a refractometer (Erma, Tokyo, Japan), respectively (Shelke, Kad, Yenge *et al.,* 2023).

Color characteristics of sweet lime

A color-scanning apparatus (Premium Color Scan, Japan) was used to measure the color of the sweet lime fruit. The hue angle and chroma were calculated using the formulas provided by Vivek *et al.,* (2018) and Barbhuiya *et al.,* (2020), as shown in Equation 27 and 28.

$$C = \sqrt{a^{*2} + b^{*2}} \quad (27)$$

$$\alpha = \tan^{-1}\left(\frac{a^*}{b^*}\right) \quad (28)$$

Where, C is chrome, α is hue angle, a* is red/green coordinate and b* is yellow/blue coordinate.

Model selection for mass prediction

The following models were presumptive when estimating the mass models for sweet lime fruit.

- The study employed single variable regression analysis to examine the correlation between the mass of sweet lime fruit and its LA, IA, and TA dimensions.
- Single or multiple variable regression analysis was employed to correlate the mass of sweet lime fruit mass with its projected areas, including P_{LA}, P_{IA}, P_{TA}, and C_{PA}.
- The mass of the sweet lime fruit is modeled as a function of the fruit's volume, assuming three different shapes: ellipsoid (V_{ellip}), oblate spheroid (V_{osp}), and prolate spheroid (V_{pro}).

Based on earlier studies, four regression models were used for the mass modeling of sweet lime fruit: linear, S-curve, quadratic, and power models, as shown in Equation 29 and 32.

$$M = b_0 + b_1X \quad (29)$$

$$M = b_0 + b_1X + b_2X^2 \quad (30)$$

$$M = b_0 + \frac{b_1}{X} \quad (31)$$

$$M = b_0X^{b_1} \quad (32)$$

Whereas, M is the mass of the fruit in grams, X is the independent variable (dimensions, volume, or projected area), and b_0, b_1, and b_2 are the parameters used for curve fitting.

Statistical analysis

The statistical measures of mean, minimum, maximum, and standard deviation for each fruit property were computed using Microsoft Excel 2007 (Microsoft

Corporation, Redmond, Washington, USA) and SPSS Statistics 20 (IBM Corporation, Armonk, New York, USA). Accurate models were then constructed based on the physical property data to determine the mass of the fruits. The model with the highest regression coefficient (R^2) was selected as the optimal mass model.

Result and Discussion

Morphological properties of sweet lime

The pulp, peel, and seed content of sweet lime fruit were extracted, and their percentages were calculated using Equations (1)–(3), while the pulp-to-peel ratio was determined through Equation (4). The mean results with standard deviation (SD) are shown in Table 1. The average percentages of pulp, peel, and seed were found to be 44.25%, 54.45%, and 1.31%, respectively, while the average pulp-to-peel ratio was 0.83. Additionally, the average peel thickness of sweet lime fruit was found to be 4.26 mm. The pulp, peel, seed content, and peel thickness of sweet lime fruit may be useful for the design and development of peeling, shredding, and crushing equipment.

Physical properties of sweet lime

Table 2 displays the physical characteristics of the sweet lime fruit. The study revealed that the mean measurements for the major axis (LA), intermediate axis (IA), and transverse axis (TA) were 78.71 mm, 77.07 mm, and 74.96 mm, respectively. Meanwhile, the average values for the geometric mean D_g, D_e, and D_a were 76.92 mm, 76.89 mm, and 76.9 mm, respectively. These diameters are essential for calculating the projected area and for designing engineering machinery used in washing, grading, sorting, and packaging (Moradi *et al.,* 2020; Pathak *et al.,* 2019*).*

P_{LA}, P_{IA}, P_{TA}, and C_{PA} were determined by computing their projected areas using Equations (8) to (11). The results indicated that the average values for P_{LA}, P_{IA}, P_{TA}, and C_{PA} were 4663.01, 4567.45, 4444.17, and 4558.21 mm^2, respectively. Meanwhile, the surface area (S_a), another important physical characteristic of sweet lime fruit, was calculated using Equation (12), with an average value of 18694.41 mm^2. These fruit areas are essential for assessing the ripeness index, transpiration rate, gas permeability, simulating mass and heat transfer, and measuring water loss (Jahanbakhshi *et al*., 2019). The shape and flowability characteristics of sweet lime fruit, such as aspect ratio and sphericity, were calculated using Equations (13) and (14), respectively. The mean values of sphericity and aspect ratio were found to be 0.98, suggesting that the sweet lime fruit has a nearly spherical shape. Mahawar *et al.* (2020) made similar observations regarding kinnow fruits. The aspect ratio and sphericity properties significantly influence the fruit's flowability. The volumes of sweet lime fruit, including V_{ellip}, V_{pro}, and V_{osp}, were calculated using Equations (15), (16), and (17), respectively. The average volumes for V_{ellip}, V_{pro}, and V_{osp} were 242.95, 254.97, and 249.79 cm^3, respectively. These volumes are crucial in various postharvest processes, such as determining heat transfer rates in refrigeration and drying operations, as well as estimating fruit density and packaging coefficients during packaging and storage (Murakonda *et al*., 2022; Roumani *et al*., 2024). The average bulk density (ρ_b) and true density (ρ_t) were found to be 449.75 and 931.41 kg/m^3, respectively. The porosity of sweet lime fruit was determined using Equation (20), yielding a value of 51.68%. Measuring the bulk density (ρ_b) and true density (ρ_t) of the fruit can aid in the development of washing and sorting machinery, as well as the design of storage structures (Mahawar *et al*., 2020). The porosity of the fruit is also essential for evaluating airflow and heat transfer characteristics (Pathak *et al.,* 2019).

Frictional properties of sweet lime

The frictional characteristics of fruit are crucial factors in the design of fruit processing equipment and operations (Murakonda *et al*., 2022; Pathak *et al*., 2020). These properties specifically influence the design of feed hoppers and mechanical conveyors (Panda *et al*., 2022).

Table 1. Morphological properties of sweet lime fruit.

Physical properties	Unit	N	Minimum	Maximum	Mean	SD
Pulp content	%	100	38.61	54.55	44.25	4.94
Peel content	%	100	43.51	60.33	54.45	5.35
Seed content	%	100	0.56	2.20	1.31	0.57
Pulp to peel ratio	-	100	0.64	1.25	0.83	0.19
Peel thickness	mm	100	2.44	6.34	4.26	1.05

N: Number of replications; SD: Standard deviation.

Table 2. Physical properties of sweet lime fruit.

Physical properties	Unit	N	Minimum	Maximum	Mean	SD
Major axis (LA)	mm	100	61.90	96.02	78.71	6.42
Intermediate axis (IA)	mm	100	60.31	94.41	77.07	6.55
Minor axis (TA)	mm	100	57.24	93.76	74.96	6.50
Arithmetic mean diameter (D_a)	mm	100	59.82	94.73	76.92	6.42
Geometric mean diameter (G_g)	mm	100	59.79	94.73	76.89	6.42
Equivalent mean diameter (D_e)	mm	100	59.80	94.73	76.90	6.42
Projected area (P_{LA})	mm^2	100	2781.38	7067.23	4663.01	793.12
Projected area (P_{IA})	mm^2	100	2709.93	6948.73	4567.45	794.39
Projected area (P_{TA})	mm^2	100	2571.99	6900.89	4444.17	791.39
Criteria projected area (C_{PA})	mm^2	100	2687.77	6972.28	4558.21	791.09
Aspect ratio (R_a)	–	100	0.94	1.00	0.98	0.02
Sphericity	–	100	0.95	1.00	0.98	0.01
Surface area (S_a)	mm^2	100	11223.18	28174.82	18694.41	3184.87
Ellipsoid volume	cm^3	100	111.83	444.81	242.95	63.81
Prolate spheroid volume	cm^3	100	120.93	455.53	254.97	65.61
Oblate spheroid volume	cm^3	100	117.83	447.90	249.79	65.04
Bulk density	kg/m^3	–	417.16	476.60	449.75	20.28
True density	kg/m^3	100	871.43	979.17	931.41	26.16
Porosity	%	–	45.31	55.91	51.68	2.58

N: Number of replications; SD: Standard deviation.

They also significantly affect the cohesion and flow of the fruit, making them essential for the design of storage structures.

The study found that sweet lime fruit exhibits good flowability, with a mean angle of repose of 6.83° (Table 3). The average coefficient of static friction for rubber, plywood, stainless steel, and aluminum sheets was 0.629, 0.523, 0.336, and 0.448, respectively (Table 3). Stainless steel showed the lowest coefficient of static friction, making it the most suitable material for constructing conveying equipment. Similar findings were reported by Motie *et al.* (2014) concerning lime fruit.

Thermal properties of sweet lime

The thermal characteristics of fruits play a vital role in the design of various processes, such as drying, cooling, freezing, sterilization, evaporation, boiling, and crystallization (Vivek *et al.*, 2018). The thermal properties of different fruits are typically determined using moisture-based regression models. In this study, the thermal properties of sweet lime fruit pulp were assessed at a moisture content of 69.74% (wet basis, w.b). Table 4 displays the thermal characteristics of sweet lime fruit. The average specific heat (Cp) value was 3.861 kJ/kg°C, which is higher than the specific heat values found in previous studies on coffee plums and Sohiong fruits (Barbhuiya *et al.*, 2020; Vivek *et al.*, 2018). Fruits with a higher Cp require more heat to be cooled or heated. Similarly, the mean value for thermal conductivity (K) was 0.581 J/m·s·°C. Thermal conductivity is crucial for determining the rate of heat transfer within food.

On the other hand, α and λ were found to be 0.00016 m^2/s and 78.52 kJ/kg, respectively, which are essential for calculating freezing and drying times. The results of this investigation are consistent with those published by Barbhuiya *et al.,* (2020) and Vivek *et al.,* (2018).

Mechanical properties of sweet lime

The mechanical characteristics of fruits are essential for designing machinery used in various processes such as peeling, shredding, handling, packaging, and cutting. These properties are also instrumental in predicting fruit quality parameters (Moradi *et al.*, 2020; Singh & Reddy, 2020). Table 4 presents the mechanical characteristics of sweet lime fruit. The analysis revealed that the average maximum penetration force was 9.44 N. Similarly, the average peak values for compression and cutting forces were 311.08 N and 148.68 N, respectively. The results are

Table 3. Frictional properties of sweet lime whole fruit.

Frictional properties	N	Minimum	Maximum	Mean	SD
Angle of repose (°)	–	3.90	9.00	6.83	1.55
Coefficient of friction					
Rubber sheet	20	0.567	0.698	0.629	0.044
Plywood	20	0.467	0.547	0.523	0.027
Stainless steel	20	0.234	0.399	0.336	0.057
Aluminum	20	0.339	0.534	0.448	0.043

N: Number of replications; SD: Standard deviation.

Table 4. Thermal and mechanical properties of sweet lime fruit.

Properties	Unit	N	Mean	Minimum	Maximum	SD
Moisture contents	%	10	86.40	88.60	87.74	0.73
Thermal						
Specific heat (Cp)	KJ/kg °C	10	3.827	3.882	3.861	0.018
Thermal conductivity (K)	J/m s °C	10	0.574	0.585	0.581	0.004
Thermal diffusivity (α)	m^2/s	10	0.00015	0.00017	0.00016	0.00001
Latent heat (λ)	KJ/kg	10	62.98	87.77	78.52	7.78
Mechanical						
Penetration force	N	10	5.50	14.88	9.44	2.49
Compression force	N	10	221.73	359.46	311.08	48.82
Cutting force	N	10	100.34	199.35	148.68	29.64

N: Number of replications; SD: Standard deviation.

consistent with data reported by Singh & Reddy (2020) for orange fruit.

Chemical properties of sweet lime

The chemical characteristics of fruits provide a reliable method for accurately evaluating fruit quality (Barbhuiya *et al*., 2020). The chemical composition of sweet lime fruit was analyzed using well-established techniques. The results, including the mean values and standard deviations (SD), are presented in Table 5. The fruit exhibited a mean moisture content of 86.40% (w.b.). For protein, fat, carbohydrates, fiber, and ash, the average values were 0.87%, 0.35%, 10.35%, 0.55%, and 0.14%, respectively. The pH level was 5.44, and the total soluble solids (TSS) had a Brix value of 11.68. The ascorbic acid (vitamin C) content was 54.50 mg/100g, highlighting the fruit's rich vitamin C concentration. These findings are consistent with the results reported by Bhaumik *et al*. (2018). The results provide a comprehensive understanding of sweet lime fruit quality, offering valuable insights for future research and practical applications in the food industry.

Color properties of sweet lime

The color of fruit significantly influences consumer preferences and serves as an indicator of its ripeness (Murakonda *et al*., 2022). Table 5 presents the color values of the sweet lime fruit. The study found that sweet lime fruit has a greenish-yellow color, with an L* value of 58.07, an a* value of -13.15, and a b* value of 51.38. The hue angle reflects the extent of light purity, while the chroma value indicates the level of color saturation and its relationship to intensity (Barbhuiya *et al*., 2020; Vivek *et al*., 2018). The analysis revealed that the hue angle and chroma values were 105.06 and 53.32, respectively.

Model selection for mass prediction of sweet lime

The study employed regression models, including linear, S-curve, quadratic, and power models, to predict the mass of sweet lime fruit. The dimensions, volume, and projected area were used as independent variables, while the fruit's weight was the dependent variable. Table 6 presents the best-fitted mass models obtained. Among

Table 5. Chemical and Color properties of sweet lime fruit.

Properties	Unit	N	Mean	Minimum	Maximum	SD
Chemical						
Protein	%	05	0.81	0.93	0.87	0.04
Fat	%	05	0.31	0.40	0.35	0.03
Carbohydrate	%	05	9.52	11.65	10.35	0.74
Fibre	%	05	0.50	0.60	0.55	0.03
Ash	%	05	0.12	0.15	0.14	0.01
Total Soluble Solids (TSS)	°Brix	05	10.87	12.30	11.68	0.42
pH	-	05	4.87	5.76	5.44	0.30
Vitamin C	mg/100 g	05	45.00	67.00	54.50	6.87
Color						
L*	-	20	45.21	66.59	58.07	6.56
a*	-	20	–18.35	–5.08	–13.15	4.21
b*	-	20	37.74	63.27	51.38	7.74
Chroma (C)	-	20	40.68	63.47	53.32	6.74
Hue angle (α)	-	20	94.63	114.34	105.06	6.11

N: Number of replications; SD: Standard deviation.

Table 6. Best-fit regression models for mass prediction of sweet lime fruit.

Parameter	Dependent	Model	R*2*	RMSE	b_0	b_1
Major axis (LA)	Mass	Quadratic	0.91	0.01325	0.1683	–0.006
Intermediate axis (IA)	Mass	Quadratic	0.93	0.01024	0.2424	–0.0078
Minor axis (TA)	Mass	Linear	0.89	0.01543	–0.3781	0.0086
Arithmetic mean diameter (D_a)	Mass	Quadratic	0.93	0.01010	0.1017	–0.0043
Geometric mean diameter (D_g)	Mass	Quadratic	0.95	0.01014	0.0358	–0.0028
Equivalent mean diameter (D_e)	Mass	Quadratic	0.93	0.01012	0.101	–0.0043
Projected area (P_{LA})	Mass	Linear	0.92	0.01067	–0.067	0.00007
Projected area (P_{IA})	Mass	Linear	0.92	0.01133	–0.0594	0.00007
Projected area (P_{TA})	Mass	Linear	0.89	0.01513	–0.0469	0.00007
Criteria projected area (C_{PA})	Mass	Linear	0.91	0.01179	–0.0593	0.00007
Surface area (S_a)	Mass	Linear	0.93	0.00974	–0.0675	0.0000092
Ellipsoid volume (V_{ellip})	Mass	Linear	0.93	0.01014	0.0509	0.0009
Prolate spheroid volume (V_{pro})	Mass	Linear	0.92	0.01130	0.0467	0.0009
Oblate spheroid volume (V_{osp})	Mass	Linear	0.93	0.01032	0.0488	0.0009

the physical dimensions, the intermediate axis (IA) was selected as the most suitable dimension for mass modeling of sweet lime fruit, with the quadratic model showing the highest R^2 value (0.93). In contrast, the geometric mean diameter (D_g), which had the highest R^2 value (0.95) for the quadratic model, was identified as the most suitable parameter among all diameters. For the projected area, P_{LA} and P_{IA} demonstrated the highest R^2 value (0.92) for the linear model. Based on their respective volumes, the ellipsoid (V_{ellip}) and oblate spheroid (V_{osp}) volumes were found to be the most appropriate for estimating the mass of sweet lime fruit, resulting in the highest R^2 value (0.93).

Finally, models based on the intermediate axis (IA), geometric mean diameter (D_g), and ellipsoid volume (V_{ellip}) were found to be the most accurate methods for estimating the mass of sweet lime fruit. Additionally, the following regression models can be applied to determine the mass of sweet lime fruit.

Best dimension-intermediate axis (IA)

$M = 0.2424 - 0.0078IA + 0.0001IA^2$, $R^2 = 0.93$.

Best diameter-geometric mean diameter (D_g).

$M = 0.0358 - 0.0028D_g + 0.00008D_g^2$, $R^2 = 0.95$

Best projected area – (P_{LA}) and (P_{IA})

$M = -0.067 + 0.00007P_{LA}$, $R^2 = 0.92$

$M = -0.0594 + 0.00007P_{IA}$, $R^2 = 0.92$

Best volume – Ellipsoid volume (V_{ellip}) and Oblate spheroid volume (V_{obl})

$M = 0.0509 + 0.0009V_{ellip,}$ $R^2 = 0.936$

$M = 0.0488 + 0.0009V_{obl}$, $R^2 = 0.933$

Conclusions

This study aimed to evaluate the engineering properties of sweet lime fruit and develop a mass model based on its physical characteristics to reduce postharvest losses. The findings include the following: The mean proportions of pulp, peel, and seeds were 44.25%, 54.45%, and 1.31%, respectively. The average values of the major axis (LA), intermediate axis (IA), transverse axis (TA), arithmetic mean diameter (D_a), geometric mean diameter (D_g), and equivalent diameter (D_e) were 78.71 mm, 77.07 mm, 74.96 mm, 76.92 mm, 76.89 mm, and 76.9 mm, respectively. The mean values for projected areas (P_{LA}, P_{IA}, P_{TA}, C_{PA}) and surface area (S_a) were 4663.01 mm^2, 4567.45 mm^2, 4444.17 mm^2, 4558.21 mm^2, and 18694.41 mm^2, respectively. The average volumes for sweet lime (V_{ellip}, V_{pro}, V_{osp}) were 242.95 cm^3, 254.97 cm^3, and 249.79 cm^3, respectively. The aspect ratio and sphericity were 0.94 and 0.95, respectively. The average bulk density and true density were 449.75 kg/m^3 and 931.41 kg/m^3. Stainless steel exhibited the lowest coefficient of static friction. Thermal properties (specific heat - Cp, thermal conductivity - K, thermal diffusivity - α, latent heat of fusion - λ) were measured as 3.861 kJ/kg°C, 0.581 J/m·s°C, 0.00016 m^2/s, and 78.524 kJ/kg, respectively. The average peak values for penetration, compression, and cutting forces were 9.44 N, 311.08 N, and 148.68 N, respectively. The chemical analysis indicated that sweet lime fruits contain a significant concentration of ascorbic acid, making them suitable as dietary supplements. The average L*, a*, and b* values for color were 58.07, –13.15, and 51.38, respectively. The mass modeling analysis determined that the linear and quadratic models were the most appropriate, with the highest R^2 values. Mass models based on the intermediate axis (IA), geometric mean diameter (D_g), and ellipsoid volume (V_{ellip}) achieved R^2 values ranging from 0.93 to 0.95. However, the study acknowledges that the effectiveness of these models depends on the unique attributes of each fruit, which may vary among different fruit varieties. Understanding the physical, thermal, mechanical, and chemical engineering properties of fruits can enhance industrial handling, postharvest processing, storage, grading, and sorting operations. Additionally, mass modeling improves the efficiency and accuracy of industrial fruit sorting.

Acknowledgment

The authors extend their appreciation to Taif University, Saudi Arabia, for supporting this work through project number (TU-DSPP-2024-79).

Author Contributions

SD, VK, GS, NKA, PKP, SK, WAA, GY, SYA: Concept development, actual experiment, manuscript writing, data analysis. MH, NA, RS, WAA, HMA, SAA, AMA: monitoring of experiment, review and editing. MKM, RS, HMA, SAA, WAA, AMA: Analysis, manuscript writing.

Conflict of Interest Statement

The authors declare no conflicts of interest.

Funding

This research was funded by Taif University, Saudi Arabia, Project No. (TU-DSPP-2024-79).

References

Abhishek, K., Vinita, R., & Ravika, R. (2017). Studies on Physical Changes in Fruit Development of Sweet Orange (Citrus sinensis (L.) Osbeck). International Journal of Pure & Applied Bioscience, 5(1): 601–612. https://doi.org/10.18782/2320-7051.2520

Azman, P. N. M. A., Shamsudin, R., Che Man, H., & Ya acob, M. E. (2020). Some Physical Properties and Mass Modelling of Pepper Berries (Piper nigrum L.), Variety Kuching, at Different Maturity Levels. Processes, 8(10): 1314. https://doi.org/10.3390/pr8101314

Barbhuiya, R. I., Nath, D., Singh, S. K., & Dwivedi, M. (2020). Mass Modeling of Indian Coffee Plum (Flacourtia Jangomas) Fruit with Its Physicochemical Properties. International Journal of Fruit Science, 20(3): 1–24. https://doi.org/10.1080/15538362.2020.1775161

Bhaumik, A., Nousheen, M., Huma, M., & Vennela, M. (2018). A potential review: phytochemical and pharmacological profile of sweet lime (mosambi fruit). Panacea Journal of Pharmacy and Pharmaceutical Sciences, *7*(4): 1–13. https://doi.org/10.1007/978-3-031-37534-7_3

Bibwe, B., Mahawar, M. K., Jalgaonkar, K., Meena, V. S., & Kadam, D. M. (2022). Mass modeling of guava (cv. Allahabad

safeda) fruit with selected dimensional attributes: Regression analysis approach. Journal of Food Process Engineering, 45(3): 1–11. https://doi.org/10.1111/jfpe.13978

Birania, S., Attkan, A. K., Kumar, S., Kumar, N., & Singh, V. K. (2022). Mass modeling of strawberry (Fragaria × Ananasa) based on selected physical attributes. Journal of Food Process Engineering, 45(5): 1–12. https://doi.org/10.1111/jfpe.14023

Hacıseferogulları, H., Gezer, I., Ozcan, M. M., & MuratAsma, B. (2007). Post-harvest chemical and physical–mechanical properties of some apricot varieties cultivated in Turkey. Journal of Food Engineering, 79(1): 364–373. https://doi.org/10.1016/j.jfoodeng.2006.02.003

Jahanbakhshi, A., Abbaspour-Gilandeh, Y., Ghamari, B., & Heidarbeigi, K. (2019). Assessment of physical, mechanical, and hydrodynamic properties in reducing postharvest losses of cantaloupe (Cucumis melo var. Cantaloupensis). Journal of Food Process Engineering, 42(5): 1–8. https://doi.org/10.1111/jfpe.13091

Khoshnam, F., Tabatabaeefar, A., Varnamkhasti, M. G., & Borghei, A. (2007). Mass modeling of pomegranate (Punica granatum L.) fruit with some physical characteristics. Scientia Horticulturae, 114(1): 21–26. https://doi.org/10.1016/j.scienta.2007.05.008

Kumari, V., Yadav, B. S., B. Yadav, R., & Nema, P. K. (2020). Effect of osmotic agents and ultasonication on osmo-convective drying of sweet lime (Citrus limetta) peel. Journal of Food Process Engineering, 43(4): 2–11. https://doi.org/10.1111/jfpe.13371

Mahawar, M. K., Bibwe, B., Jalgaonkar, K., & Ghodki, B. M. (2019). Mass modeling of kinnow mandarin based on some physical attributes. Journal of Food Process Engineering, 42(5): 1–11. https://doi.org/10.1111/jfpe.13079

Mahawar, M. K., Jalgaonkar, K., & Bhushan, B. (2020). Development of composite mechanical peeler cum juice extractor for kinnow and sweet orange. Journal of Food Science and Technology, 57: 4355–4363. https://doi.org/10.1007/s13197-020-04472-9

Mondal, N. K., Basu, S., Sen, K., & Debnath, P. (2019). Potentiality of mosambi (Citrus limetta) peel dust toward removal of Cr(VI) from aqueous solution: an optimization study. Applied Water Science, 9(4): 1–13. https://doi.org/10.1007/s13201-019-0997-6

Moradi, M., Balanian, H., Taherian, A., & Mousavi Khaneghah, A. (2020). Physical and mechanical properties of three varieties of cucumber: A mathematical modeling. Journal of Food Process Engineering, 43(2): 1–8. https://doi.org/10.1111/jfpe.13323

Motie, J., Miraei, A. S. H., Abbaspour, F. M. H., & Emadi, B. (2014). Modeling physical properties of lemon fruits for separation and classification. International Food Research Journal, 21(5): 1901–1909.

Mukama, M., Ambaw, A., & Opara, U. L. (2020). Thermophysical properties of fruit—a review with reference to postharvest handling. Journal of Food Measurement and Characterization, 14(5): 2917–2937. https://doi.org/10.1007/s11694-020-00536-8

Murakonda, S., Patel, G., & Dwivedi, M. (2022). Characterization of engineering properties and modeling mass and fruit fraction of wood apple (Limonia acidissima) fruit for post-harvest processing. Journal of the Saudi Society of Agricultural Sciences, 21(4): 267–277. https://doi.org/10.1016/j.jssas.2021.09.005

Panda, T. C., Thota, N., Dwivedi, M., Pradhan, R. C., & Seth, D. (2022). Mass modeling of engineering properties and characterization of Kadamb fruit (Neolamarckia cadamba): An underutilized fruit. Journal of Food Process Engineering, 45(11): 1–12. https://doi.org/10.1111/jfpe.14160

Pathak, S. S., Pradhan, R. C., & Mishra, S. (2019). Physical characterization and mass modeling of dried Terminalia chebula fruit. Journal of Food Process Engineering, 42(3): 1–10. https://doi.org/10.1111/jfpe.12992

Pathak, S. S., Pradhan, R. C., & Mishra, S. (2020). Mass modeling of Belleric Myrobalan and its physical characterization in relation to post-harvest processing and machine designing. Journal of Food Science and Technology, 57(4): 1290–1300. https://doi.org/10.1007/s13197-019-04162-1

Patil, M., Shinde, S., & Panchal, V. (2017). Comparative growth, quality and yield performance study of sweet orange genotypes under rainfed vertisol of Marathwada. International Journal of Chemical Studies, 5(4): 157–160.

Roumani, M., Remmani, R., Miladi, M., Abu-Khalaf, N., & Canales, A. R. (2024). Physical properties and mass models of Deglet Noor and Arichti semi-dry Algerian date fruits: A comparative study. Food Science and Nutrition, 12(4): 2886–2895. https://doi.org/10.1002/fsn3.3969

Sanganamoni, S., Kancherla, S., Pedapati, A., Akki, S., & Patel, J. (2024). Physical characterization and development of mathematical models for predicting mass and area of oil palm fruits. Journal of Food Process Engineering, 47(1): e14512. https://doi.org/10.1111/jfpe.14512

Shariq, M., & Sohail, M. (2019). Citrus limetta peels: a promising substrate for the production of multienzyme preparation from a yeast consortium. Bioresources and Bioprocessing, 6(1): 2–15. https://doi.org/10.1186/s40643-019-0278-0

Shelke, G., Pandiarajan, T., & Modi, R. (2018). Effect of Moisture Content on Engineering Properties of Chickpea Seed. Research Journal of Agricultural Sciences, 10(1): 180–184. https://www.researchgate.net/publication/303437276

Shelke, G., Kad, V., Yenge, G., Desai, S., & Kakde, S. (2020). Utilization of jamun pomace as functional ingredients to enhance the physico-chemical and sensory characteristics of ice cream. Journal of Food Processing and Preservation, 44(10): 1–8. https://doi.org/10.1111/jfpp.14736

Shelke, G., Kad, V., Pandiselvam, R., Yenge, G., Kakade, S., Desai, S., Kukde, R., & Singh, P. (2023). Physical and functional stability of spray-dried jamun (Syzygium cumini L) juice powder produced with different carrier agents. Journal of Texture Studies, 1: 1–11. https://doi.org/10.1111/jtxs.12749

Shelke, G., Kad, V., Yenge, G., Kukde, R., Kakade, S., Al-Dalain, S. Y., Haddad, M., Abdeen, A., et al. (2023). Physicochemical attributes, antioxidant activity, and sensory responses of low-fat cheese supplemented with spray-dried Jamun juice (Syzygium cumini L.) powder. Frontiers in Sustainable Food Systems, 7(8): 1–12. https://doi.org/10.3389/fsufs.2023.1243477

Shousha, E. R., Tayel, S. A., & Ghanem, T. H. (2024). Mass modeling of pomegranate fruit using some physical properties. Al-Azhar Journal of Agricultural Engineering 6, 6(1): 1–10.

Singh, K. K., & Reddy, B. S. (2020). Post-harvest physico-mechanical properties of orange peel and fruit. Journal of Food Engineering, 73: 112–120. https://doi.org/10.1016/j.jfoodeng.2005.01.010

Tewari, R., Kumar, V., & Sharma, H. K. (2019). Physical and chemical characteristics of different cultivars of Indian gooseberry (Emblica officinalis). Journal of Food Science and Technology, 56(3): 1641–1648. https://doi.org/10.1007/s13197-019-03595-y

Tomar, M. S., & Pradhan, R. C. (2022). Prediction of mass-based process designing parameters of amla fruit using different modeling techniques. Journal of Food Process Engineering, 45(8): 1–7. https://doi.org/10.1111/jfpe.14039

Vivek, K., Mishra, S., & Pradhan, R. C. (2018). Physicochemical characterization and mass modelling of Sohiong (Prunus nepalensis L.) fruit. Journal of Food Measurement and Characterization, 12(2): 923–936. https://doi.org/10.1007/s11694-017-9708-x

Yıldız, G., Izli, N., Unal, H., & Uylaser, V. (2015). Physical and chemical characteristics of goldenberry fruit (Physalis peruviana L.). Journal of Food Science and Technology, 52(4): 2320–2327. https://doi.org/10.1007/s13197-014-1280-3

Younis, K., Islam, R. U., Jahan, K., Yousuf, B., & Ray, A. (2015). Effect of addition of mosambi (Citrus limetta) peel powder on textural and sensory properties of papaya jam. Cogent Food & Agriculture, 1(1): 1023675. https://doi.org/10.1080/23311932.2015.1023675